ELSEVIER

Computational and Theoretical Polymer Science 10 (2000) 221–233

Computational and Theoretical Polymer Science

Microstructure of 2,3 erythro di-isotactic polynorbornene from atomistic simulation

S. Ahmed[1], P.J. Ludovice*, P. Kohl

School of Chemical Engineering, Georgia, Institute of Technology, Atlanta, GA 30332-0100, USA

Received 16 April 1999; received in revised form 8 September 1999; accepted 9 September 1999

Abstract

A new RIS model was developed for erythro di-isotactic polynorbornene that included long-range steric interactions that are needed to properly model its conformation. These interactions were included by extracting RIS states from an approximate energy state map for the heptamer of this polymer. The RIS model predicted a novel helix-kink conformation for this polymer in which helices were occasionally disrupted by a backbone kink and a value of approximately 1.9 for the exponent "a" from the Mark–Houwink–Sakurada equation at the θ condition. These RIS results were consistent with independent single chain Monte Carlo simulations and were also used to generate bulk periodic structures of this polymer. The results of these simulations compare well to both experimental viscometry and wide angle X-ray diffraction results for two polymer samples synthesized using Pd and zirconocene homogeneous polymerization catalysts. These results indicated that the likely stereochemical configuration for polymers produced using these catalysts is the erythro di-isotactic form. They also suggested that polymers of similar structure such as *cis* poly(*t*-butyl acetylene) may also adopt this kink-helix conformation.

Keywords: Polynorbornene; Atomistic simulation; Rotational isomeric states

1. Introduction

The bi-cyclic variation of polynorbornene is a polymer currently under investigation for a number of applications, including deep ultra-violet photoresists and interlevel dielectrics in microelectronics applications [1–6]. The 2,3-norbornene monomer undergoes a vinyl-like polymerization that retains the bi-cyclic conformation in the backbone of the resulting polymer as seen in Fig. 1. This is unlike the commonly employed Ring Opening Metathesis Polymerization (ROMP) mechanism which retains only a single ring in the polymer backbone [7,8]. This polymer is currently being developed for inter-level dielectric applications by the BF Goodrich Company under the trade name Avatrel® dielectric polymer. Polynorbornene has excellent dielectric properties and both processing and potential cost advantages over other materials currently being used as inter-level dielectrics [1,9]. The high barrier to backbone rotation produces a high glass transition temperature which allows the use of this polymer in the high temperature processing steps employed in microelectronics fabrication. This lack of segmental mobility coupled with a lack of a strong dipole produces a low dielectric constant, which makes this material a good dielectric insulator. However, the bi-cyclic backbone structure makes it difficult for direct experimental characterization of the polymer microstructure using 2D NMR [1,10,11]. Therefore, we used a combination of molecular modeling and experiment to determine the likely microstructure of this polymer. This work utilized a customized force field for poly(norbornene) developed previously using semi-empirical, Hartree–Fock, and Density Functional Theory quantum calculations [12]. This force field was developed to account for the high level of ring strain and steric hindrance of the backbone that occurs in poly(norbornene). Generic force fields are not parameterized for bi-cyclic structures, and the optimized parameters for both the bicycloheptane geometry as well as the backbone torsional barrier differed from generic force field parameters.

Based on NMR experiments carried out by researchers at the BF Goodrich Corporation, poly(norbornene) is believed to undergo 2,3 exo–exo polymerization (Fig. 1), regardless of the homogeneous polymerization catalyst used [1]. The hydrogens that occupy the endo positions on carbons 2 and 3 extend below the plane of the polymer backbone and are not pictured in Fig. 1. We hypothesize that different catalyst

* Corresponding author.
E-mail address: pete.ludovice@che.gatech.edu (P.J. Ludovice).
[1] Current address: Merck & Company, Whitehouse Station, NJ, USA.

1089-3156/00/$ - see front matter
PII: S1089-3156(99)00083-5

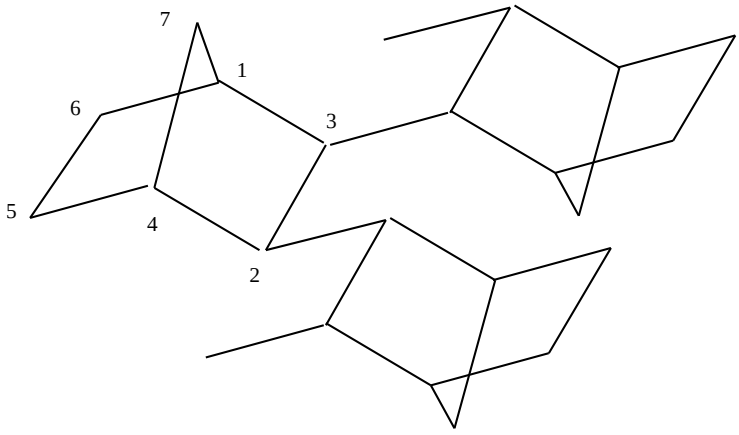

Fig. 1. Structure of polynorbornene showing 2,3 exo–exo enchainment. This particular trimer is erythro di-isotactic isomer.

systems produce different stereochemical configurations and this gives rise to different properties [13,14]. It is presumed that the zirconocene catalyst analyzed by Kaminsky and co-workers [15,16], and the palladium catalyst developed by the BF Goodrich corporation [17] both produce the highly stereo-regular 2,3 erythro di-isotactic polynorbornene. Our hypothesis is based on the fact that both these polymers have identical Wide Angle X-ray Diffraction (WAXD) patterns and they are both intractable or insoluble in organic solvents under typical conditions. In the 2,3 erythro di-isotactic configuration, the bridging carbons (carbon #7) point in alternating directions when the polymer is in the all *cis* extended conformation (see Fig. 1). Fig. 2 contains a heptamer of the erythro di-isotactic configuration, which is analyzed in this work. Preliminary WAXD results for the Pd catalyst are identical to Kaminsky's WAXD for polymer produced from the ziconocene catalyst that indicates that poly(norbornene) produced from these catalysts have the same or similar structure [18]. Although other current work is focused on the connection between various stereochemical configurations and catalysts [13], the microstructure of the erythro di-isotactic isomer of polynorbornene, in the glassy state, is investigated here. The comparison of simulation results to experiment is used to test our hypothesis that this is the likely stereochemical configuration for poly(norbornene) obtained with the Pd and zirconocene catalysts above.

2. Results and discussion

2.1. Rotational isomeric states model

A Rotational Isomeric States [19,20] (RIS) model was developed for 2,3 erythro di-isotactic polynorbornene. RIS models approximate the conformation space of the polymer chain as a set of low energy conditional torsional states. The RIS model, in a typical implementation, is a first-order Markov model in which the probability of any backbone torsional angle occurring is dependent on the state of the previous rotatable bond. Using matrix techniques, these models can be used to elucidate the microstructure of isolated polymer chains [19,20] and can also be used to generate the starting conformations for subsequent minimization or dynamics studies in periodic boundary conditions [21–23]. This model assumes a first-order Markov Process in which the occupation of a given torsional state is a function of only the previous state. This means that the energetic

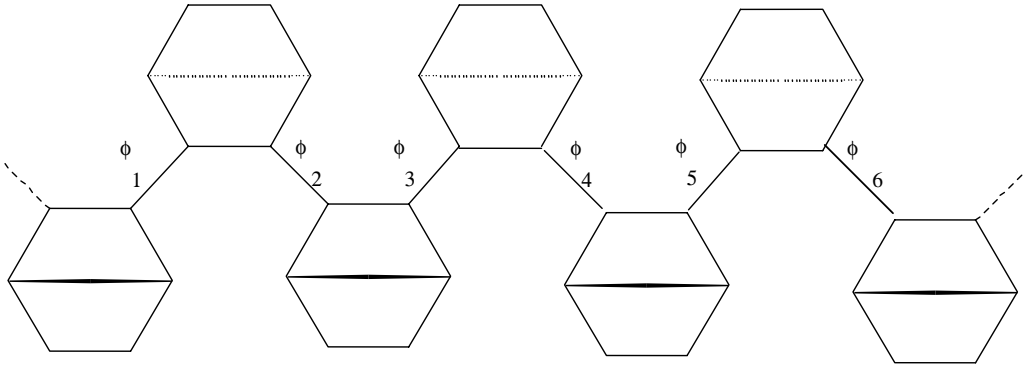

Fig. 2. 2,3 erythro di-isotactic polynorbornene heptamer. The numbering scheme for the rotatable backbone torsions in the heptamer is shown.

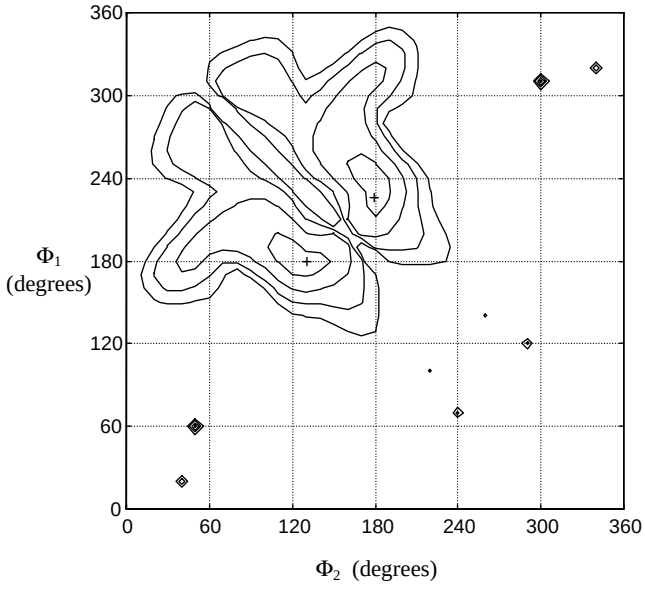

Fig. 3. Potential energy contour plot for torsion angles ϕ_1 and ϕ_2 in a trimer. The minima are marked with a + symbol. Contour levels are at 4,7,10 and 13 kcal/mol above the minimum.

states are determined by specifying two adjacent torsional states and described by a second-rank transition probability tensor. The interactions that determine these states are called second order interactions within the RIS framework because they involve two adjacent torsion angles. While the formulation of a second order Markov model that involves third-order RIS interactions is possible, it is impractical given the mathematical complexity involved for polymers. The typical RIS model incorporates only second-order interactions by using a serial product of large second-rank tensors that produce an ensemble average of geometric properties over all the rotational isomeric states. To our knowledge explicit inclusion of third order RIS interactions has not been used for large polymers because this would involve a product of generator tensors of rank three. Rather, we have included these higher order interactions in an approximate fashion as described below.

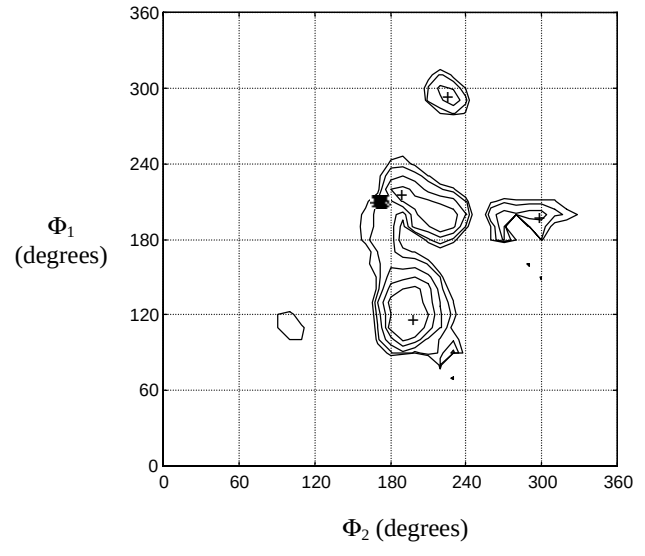

Fig. 4. Potential energy contour plot for torsion angles ϕ_3 and ϕ_4 in a heptamer. The minima are marked with a + symbol and the group of dots indicates the region in which all the Boltzmann Jump minima were clustered. Contour levels are at 3,6,9 12 and 14 kcal/mol above the minimum.

The bulky nature of the bicycloheptane backbone group makes these long range intramolecular effects significant. This is clear from a comparison of conformational energy state maps for a trimer and heptamer of polynorbornene. Fig. 3 shows a potential energy contour as a function of two backbone torsion angles using a trimer of di-isotactic polynorbornene. A trimer of polynorbornene contains two rotatable backbone torsion angles and is the smallest oligomer that can be used to characterize the RIS states. The energies used to produce the contours in Fig. 3 were calculated using version 1.5 of the Cerius$^{2®}$ program from Molecular Simulations Inc. [24]. Energies were calculated at increments of 10° and utilized the aforementioned custom force field [12]. The internal energy was minimized with respect to all other degrees of freedom in the trimer other than the two torsion angles. In this RIS treatment we assume that the bond connecting atoms 2 and 3 is non-rotatable. The highly strained bicycloheptane group makes this a reasonable assumption although this is not always the case for more flexible rings such as those found in the amino acid proline. Fig. 3 illustrates the classic symmetry of the typical RIS model. In this particular case the symmetry is about the normal to the diagonal ($\Phi_1 = -\Phi_2$) as opposed to the diagonal ($\Phi_1 = \Phi_2$) simply because of the anti-symmetric definition of the torsional angles used. We used the same reference for the definition of the torsional angles as that used in the Cerius$^{2®}$ program. For more flexible polymers, such as poly(olefins), the energy map of a segment containing two rotatable bonds is sufficient to characterize the conformational behavior of the entire polymer chain through the RIS model. This occurs because long range energetic interactions along the polymer chain are relatively small and do not significantly change the RIS state map like the one seen in Fig. 3. However the bulky nature of the bicycloheptane group in the backbone of poly(norbornene) suggests that long-range energetic effects may be more significant. Calculations of the same RIS state map pictured in Fig. 3 for the poly(norbornene) pentamer and heptamer show drastically different behavior. Fig. 4 is the RIS state map for the heptamer of erythro di-isotactic poly(norbornene), whose structure is pictured in Fig. 2. These energy calculations were carried out in a similar fashion to the trimer calculations except that the energy was minimized at each point with respect to the four external torsion angles (angles 1, 2, 5 and 6 in Fig. 2). Angles 1 and 2 on the axes in Fig. 4 are the internal angles only, and correspond directly to angles 3 and 4 from Fig. 2. Because the four additional internal angles are in local minima only, the energy map in

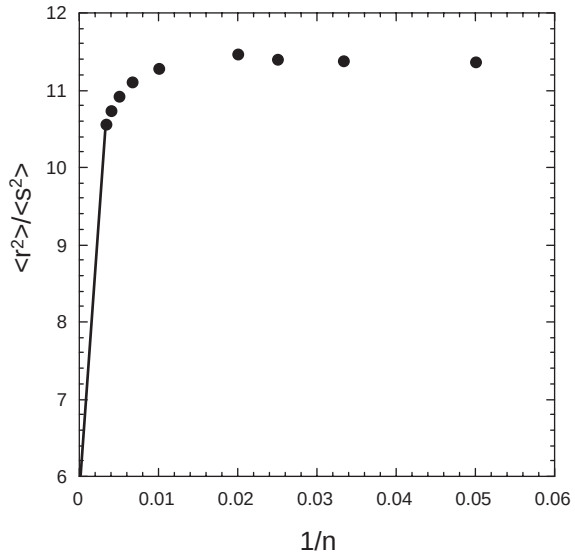

Fig. 5. The ratio of end–end distance to radius of gyration plotted against inverse number of bonds from the RIS model.

Fig. 4 is only an approximate characterization of the energetic states. This approximation is responsible for the loss of the typical symmetry in this plot. A more appropriate map is obtained by finding the global energy minima for structures with fixed internal angles (3 and 4). Better still, integration of the Boltzmann factor for all conformations with fixed internal angles would account for the entropy of these additional degrees of freedom. These approaches would require exhaustive searches and enumerations over all conformational variations of these four angles. If local minima were obtained for conformations involving the additional four angles at the same resolution (10° increments) as the two internal angles, this would require 1.67×10^6 times the computational resources of the approximate approach used in Fig. 4. Currently the calculation in Fig. 4 requires approximately one day on a workstation so the more detailed calculation was infeasible. However, we are currently investigating the symmetry of this molecule in order to reduce the resolution of such a search without neglecting important conformations.

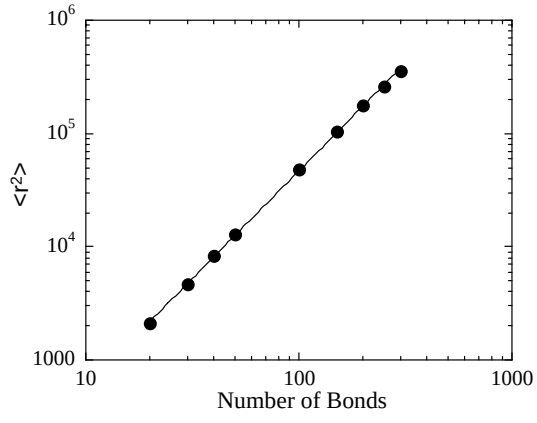

Fig. 6. Radius of Gyration plotted against the number of bonds from the RIS model on a double logarithm scale.

Despite the approximate nature of the energy map in Fig. 4, various structural features are readily apparent. The most prominent feature is the lowest energy state at $\Phi_1 \approx 120°$ and $\Phi_2 \approx 200°$. Despite the fact that this is the lowest-energy state, this state is an artifact of the approximate method used to obtain this map. This state indicates that if a backbone torsion adopts an angle of approximately 120° the following angle is very likely to adopt a value of 200°. The map shows that essentially no angle is likely to produce a subsequent angle of 120° as seen in the absence of any reasonable low energy minima at $\Phi_1 \approx 120°$. This energy map contains these artifacts because any state is dependent on the local minimum in which the other four external angles reside. This state occurs because the other four angles associated with these values of the internal angles happen to be in a very low energy minimum, while the other states could have found higher energy minima.

The next lowest state is at $\Phi_1 \approx 200$ and $\Phi_2 \approx 200°$. Given the similarity of these two angles this state involves the repetition of approximately the same angle over and over again. Minimized structures with these angles suggest an incommensurate helix that adopts a repeated angle in the vicinity of 200°. We confirm that this helical structure is in the vicinity of this state by carrying out a Monte Carlo (MC) search on the stereo-regular heptamer as explained below. The heptamer conformations obtained from this simulation are all clustered in the vicinity of the helical state seen in Fig. 4.

There are two other relatively low-energy states that occur on the energy map in Fig. 4. The first occurs at $\Phi_1 \approx 200$ and $\Phi_2 \approx 300°$ which is a state that represents a deviation from the helical conformation to a larger angle. The other state occurs at approximately $\Phi_1 \approx 300$ and $\Phi_2 \approx 200°$ which represents the chain jumping back into the helical conformation. These low energy states in the material indicate a polymer chain that adopts a helical conformation that is occasionally disrupted by a kink. This kink consists of the state at $\Phi_1 \approx 200$ and $\Phi_2 \approx 300$ followed by the state at $\Phi_1 \approx 300$ and $\Phi_2 \approx 200°$.

By integrating the Boltzmann factor, in the vicinity of the three local energy states described above, we can obtain probability weighting for an RIS model. Because the energy map on which this model is based is approximate, we will use $\Phi_1 = 200$ and $\Phi_2 = 300°$ as the energy states. The transition state matrix (U) for this RIS model is:

$$\mathrm{U} = \begin{array}{c} \\ \phi_1 = 200^o \\ \phi_1 = 300^o \end{array} \begin{array}{c} \begin{array}{cc} \phi_2 = 200^o & \phi_2 = 300^o \end{array} \\ \begin{bmatrix} 1 & 0.03385 \\ 1 & 0 \end{bmatrix} \end{array} \tag{1}$$

indicating that 3.385% of the angles at 200° will jump out of the helix conformation. This RIS model can be used with the geometry of the polymer chain determined from previous quantum calculations [12] to obtain the scaling of radius of gyration and end-to-end distance as a function of molecular

Table 1
Probability of one of more kinks occurring in a poly(norbornene) oligomer based on RIS model

Degree of polymerization	Probability of one or more kinks
7	0.1802
11	0.2824
15	0.3719
19	0.4502

weight by using the matrix generation scheme of the RIS model [19,20]. Note that this RIS scheme assumes that the bond in the bicycloheptane group is non-rotatable and makes no contribution to the chain flexibility. This assumption is justified by the rigid nature of the bicycloheptane group as stated above.

Fig. 5 is a plot of the ratio of the unperturbed mean squared end-to-end distance $\langle r_0^2 \rangle$ to the unperturbed radius of gyration $\langle s_0^2 \rangle$ vs. the inverse of the degree of polymerization ($1/n$) from the approximate RIS model. The value of this ratio is approximately constant at a value of 11.5 and then decreases as the chain approaches infinite length. In the limit of infinite chain length this ratio approaches a value of 12 for a rigid rod, 6 for a random coil or 2 for a collapsed coil that can occur in globular proteins. Given the presence of the kink we postulate that this polymer will behave like a random coil in the infinite molecular weight limit. The line in Fig. 6 simply connects the last simulated point with this limit. Although our calculations have not reached this limiting behavior, the line suggests that this postulate is not unreasonable. Based on the RIS model, the polymer is presumed to be a helix with the occasional kink. A perfect helix would have a ratio of slightly less than 12 at low molecular weights due to the finite cross-section of the polymer caused by the helical windings. However in the limit of truly infinite molecular weight the cross-section of the helix would be infinitesimal compared to the length, so this would approach an infinitely thin rod which has a value of 12 for this ratio. The stereo-regular poly(norbornene) pictured in Fig. 5 is a helix with the occasional kink. At low molecular weight the polymer is predominantly helical. Even the averaging of the occasional kink does not reduce the ratio to much below 12 because the kink has a limited range of angles such that a few kinks do not significantly deviate the polymer chain from its initial persistence direction. However, as more than a few kinks are incorporated the chain begins to behave like a random coil. From calculations described below using the RIS model (see Table 1), the average number of kinks that occur in 100 repeat units is slightly less than three. This is not sufficient to cause significant deviation from an elongated conformation. However, at higher degrees of polymerization, the polymer chain begins to slowly transition to random coil behavior. This is why the ratio in Fig. 5 begins to decrease at $1/n = 0.01$ ($n = 100$). It will require a very large degree of polymerization for this ratio to approach the theoretical value of six.

Fig. 6 contains a log–log plot of the ratio of the radius of gyration vs. the degree of polymerization calculated from the RIS model. The slope of the best-fit line through the points in this plot is 1.927 ± 0.014 which indicates that the radius of gyration scales with the degree of polymerization to approximately the 1.9 power. The reported range of this slope is the 90% confidence interval for this value assuming a Normal distribution of the error about the best-fit line. This scaling exponent approaches two as the polymer geometry approaches a rigid rod shape where the dimension of the polymer chain scales linearly with the degree of polymerization. This limit occurs with rigid rods, but this case illustrates that it can occur with less regulars geometric shapes, such as the kinked-helix produced by these calculations. For a perfect helix the value of this exponent would be two, but this value is less than two due to the presence of the kinks in the chain backbone. However, since the range of the degree of polymerization (n) is the same for both Figs. 5 and 6 the exponent is only slightly less than two. This occurs because the ratio of mean squared end-to-end distance to the mean squared radius of gyration only varies be from approximately 11.5 to 10.5, indicating that the polymer still adopts a relatively elongated average conformation over this range of n.

Using the universal viscosity law we may relate the scaling of the radius of gyration with molecular weight obtained from Fig. 6 to a similar scaling of the intrinsic viscosity $[\eta]$ with molecular weight. This can provide us with some experimental validation. However, there is some question as the applicability of the universal viscosity law since it is based on the Einstein viscosity model [25,26], which assumes spherically shaped particles in the solution. To address this we will assume that polymers, most of which do not adopt an instantaneous shape similar to a sphere can sweep out an effective sphere as they rotate in solution. From the Einstein model, one can express the intrinsic viscosity $[\eta]$ as a function of the effective volume of the sphere V_e. This relationship is given Eq. (2)

$$[\eta] = 2.5 \frac{N V_e}{M} \tag{2}$$

where N is Avogadro's number and M is the molecular weight. The universal viscosity law is typically derived by assuming that the sphere volume can be expressed using an effective radius R_e, that is proportional to the root-mean-squared end-to-end distance of the polymer chain. Here we assume such a relationship in Eq. (3)

$$R_e = \alpha \gamma \langle r_0^2 \rangle^{1/2} \tag{3}$$

where α is the solvent expansion parameter that describes the expansion of the chain above its θ condition value due to interaction with solvent. The parameter γ is the ratio of the radius of the effective sphere swept out by the rotating polymer to the actual average end-to-end distance that the polymer adopts instantaneously. We assume here that γ is not a function of molecular weight and only depends on the

conformational behavior of the chain. One might expect that γ for a random coil is slightly larger than that of a rigid rod because the rigid rod most likely does not sweep out all of the three-dimensional (3D) space available to it. We also assume that α is independent of molecular weight. This is reasonable because Flory Krigbaum theory can be used to estimate that α scales as $M^{0.1}$ at high molecular weight [27]. Assuming that the volume in Eq. (2) is given by the volume of a sphere with the effective radius given in Eq. (3), we obtain Eq. (4)

$$[\eta] = 2.5\gamma^3 \frac{4\pi N}{3} \left(\frac{\langle r_0^2 \rangle}{M} \right)^{3/2} M^{1/2} \alpha^3 \tag{4}$$

By combining some of the constants we obtain the commonly used form of the universal viscosity law [19] given in Eq. (5)

$$[\eta] = \Phi \left(\frac{\langle r_0^2 \rangle}{M} \right)^{3/2} M^{1/2} \alpha^3 \tag{5}$$

where Φ is an empirical constant. In this case the effect of the non-spherical shape of the chain (contained in γ) does not effect the scaling of the intrinsic viscosity with molecular weight, it only affects the pre-factor Φ. At the θ condition where $\alpha = 1$, or in the high molecular weight limit where the dependence of α on M is very weak, we have the following scaling law

$$[\eta] \propto \left(\frac{\langle r_0^2 \rangle}{M} \right)^{3/2} M^{1/2} \tag{6}$$

Empirical observation has validated this scaling for molecules of arbitrary shape [28]. This probably occurs because non-spherical molecules sweep out an effective sphere as assumed above. We typically assume that random coils are spherical in shape, but this is only true for an external reference frame. Even random coils appear to be non-spherical when observed in their internal reference frame. The instantaneous shape of a random coil polymer is more like an oblate or prolate spheroid [29,30]. Given this, we will use Eq. (6) across the entire range of polymer shapes from random coils to rigid rods. For a random coil the mean squared radius of gyration is proportional to the molecular weight and for a rigid rod it is proportional to the square of the molecular weight. From this we obtain the limits in scaling of intrinsic viscosity with molecular weight at the θ condition.

$$[\eta] \propto M^{1/2} \text{(random coil)}. \tag{7}$$

$$[\eta] \propto M^2$$
(elongated structure where size increases linearly with n) (8)

This exponent, typically referred to as “a” in the Mark–Houwink–Sakurada empirical relationship between intrinsic viscosity and molecular weight, varies between 1/2 for a random coil in a θ solvent and approximately 0.8 in a good solvent. Eq. (8) is dependent on our previous justification for using Eq. (6) with rigid elongated structures. Additional validation of the scaling obtained in Eq. (8) is seen in the results of Prager, who found that intrinsic viscosity of rigid dumbbell shaped molecules scaled in the same quadratic fashion [31]. After substituting the slope of 1.927 from Fig. 6 into Eq. (6) we obtain an exponent of 1.9 ± 0.2 for the scaling of intrinsic viscosity with molecular weight. This can be compared to the experimental results below.

2.2. Monte Carlo simulations

Two types of MC simulations were carried out on 2,3-erythro di-isotactic polynorbornene to validate the conformational behavior derived from the RIS model above. This validation is important because the RIS model is based on an approximate energy map that does not completely sample the conformational space of the heptamer of polynorbornene. First, a conformational search was conducted on a di-isotactic polynorbornene heptamer. Using the Boltzmann Jump algorithm developed by Venkatachalam [32]. The Boltzmann Jump algorithm is particularly useful for sampling local conformational minima. It carries out a number of random torsion angle perturbations using the MC Metropolis algorithm [33] until the molecule is sufficiently far from its previous point in conformation space to potentially be in another local energy minimum. At this point an energy minimization is carried out to produce a collection of local energy minima. We employed this algorithm to produce 3000 different energy minimized structures using 50 MC steps each before energy minimization. The conformers were energy minimized to a root mean square (rms) force of 0.1 kcal/mol/Å. We employed a temperature of 5000 K in the MC search to ensure a broad sampling of phase space. The high temperature is employed to assist the structure in moving to completely different areas of phase space, but since the final structures undergo energy minimization, they in no way reflect the conformational distribution at this artificially elevated temperature. Despite the high temperature employed, all of the conformations produced resided in the vicinity of the helical conformation as indicated by the darkened region in Fig. 4. What appears to be a large dot in Fig. 4 is actually a tight cluster of points generated from the Boltzmann Jump simulation. The Boltzmann Jump calculations verify the occurrence of the helical state in Fig. 4. This is essentially the same helical structure that may occur in substituted polyacetylenes as we discuss below.

Second, a Metropolis-MC [33] simulation incorporating the pivot algorithm [34] followed by energy minimization was used to simulate isolated chains of polynorbornene. No correction was applied for the potential conformational bias caused by the minimization step, but without the minimization step the acceptance ratio was prohibitively low. This is to be expected at the low temperature (300 K) used in these

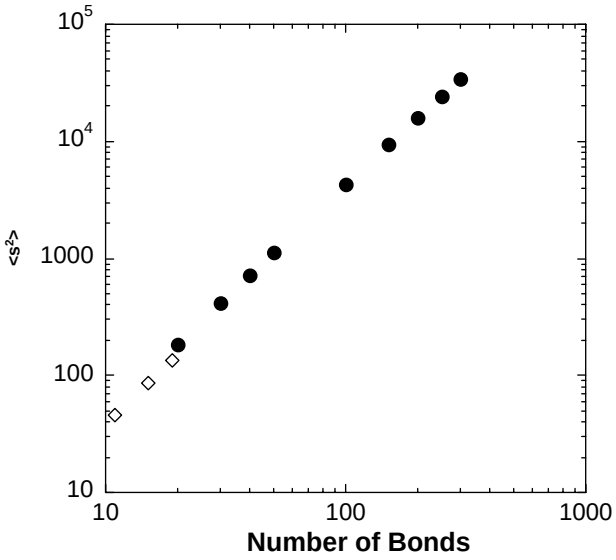

Fig. 7. Comparison of Monte Carlo results for erythro di-isotactic polymer (diamonds) and RIS calculations for the same stereochemical isomer (filled circles).

simulations for sterically hindered polymers such as poly(norbornene) [35]. With the minimization step, the acceptance ratio was approximately 2%. Starting from an initial extended conformation, a random torsional perturbation, using a random uniform distribution, is applied to one rotatable bond, this is followed by 4000 steps of energy minimization using the BFGS [36] algorithm. The assumption that isolated chains are sufficient to describe the structure of this polymer is justified by the fact that the bulky backbone of the polymer makes the intramolecular interactions much stronger than the intermolecular ones. It is assumed that the polymer conformations are determined primarily by the intramolecular torsional barriers and steric hindrance, while the surrounding polymer produces a minor structural perturbation. Similar simulation approaches have been shown to faithfully reproduce experimental data, albeit for simpler polymers [35,37,38]. This single-chain assumption is justified by the extremely high torsional barriers for this polymer. Due to the computational requirements of the energy minimization in this simulation, small oligomers were simulated corresponding to degrees of polymerization of 11, 15 and 19. These three oligomers were simulated for 1000 total steps, and resulted in 15–20 accepted structures. A direct comparison can also be made between the results of the MC and RIS simulations and this is seen in Fig. 7. Good agreement is observed between the MC and RIS results further validating the approximate RIS model. Fig. 7 indicates that both the RIS and MC models suggest that the radius of gyration scales with the molecular weight to approximately the 1.9 power. The slope obtained for the MC simulation is 1.95 ± 0.219 where this range is the 90% confidence interval on the slope in Fig. 7. After substituting this value of the slope into equation two, the MC models predict that intrinsic viscosity varies with the molecular weight to the 1.9 ± 0.3 power, which compares well to the value obtained from the RIS model.

Since this is quite close to the elongated rod limit of two, the overall dimensions of this polymer increase almost linearly with degree of polymerization. A perfect helix would approach this limiting exponent of two as well, however, the conformations sampled in the MC model were not perfect helices and appeared to have helical character with kink-like conformations suggested by the RIS model. This occurred despite the failure of the Boltzmann Jump calculations to sample the kink architecture. The better sampling of this MC procedure is due in part to the longer chains in the simulation. The probabilities from the RIS statistical weight matrix in Eq. (1) can be used to estimate the probability of occurrence of one more kinks in a given oligomer. This can be calculated from the conditional probabilities of a helix angle ($\phi_1 = 200°$) transitioning to a kink angle ($\phi_2 = 300°$). This probability (p_{23}) is 0.032745 as seen in equation one, and the corresponding probability that a helix angle is followed by another helix angles is 0.96755 and is denoted p_{22}. We may estimate the *a priori* probabilities that a given angle is at the helix or kink value by recalling that all kink angles must follow a helix angle. This allows us to equate the *a priori* probability of the occurrence of a kink angle (P_{300}) with the fractions of diads (or adjacent pairs of monomeric units) that contain a helix angle followed by a kink angle. This equality is expressed in Eq. (9)

$$P_{300} = 1 - P_{200} = P_{200}p_{23} \tag{9}$$

where P_{200} and P_{300} are the a priori probabilities of the occurrence of $\phi = 200$ and $\phi = 300°$ in the backbond torsion angle distribution. These are also equal to the fraction of helix and kink angles, respectively. Solving Eq. (5) we obtain $P_{200} = 0.9683$ and $P_{300} = 0.0317$ for the a priori probabilities. By employing the first order Markov model inherent in the RIS model we may calculate the probability of one of more kinks (P_{kinks}) occurring in an oligomer of degree of polymerization n that contains $n - 1$ angles. This can be done by subtracting the probability of no kinks occurring from 1 as in Eq. (10)

$$P_{\text{kinks}} = 1 - P_{\text{no kinks}} = 1 - P_{200}p_{22}^{n-2}. \tag{10}$$

These values are listed in Table 1 and they indicated that the likelihood of even one kink occurring in the heptamer is relatively low. This explained the fact that the Boltzmann Jump simulation did not encounter any kinks while the larger oligomers did.

2.3. Viscometry experiments

Validation that the intractable polynorbornene produced via the zirconocene or Pd catalyst can, in principle, be made by comparing the results of the RIS and MC calculations with viscometry measurements made on these polymers. Recall that we are presuming that the zirconocene and Pd catalysts produce essentially the same stereochemical

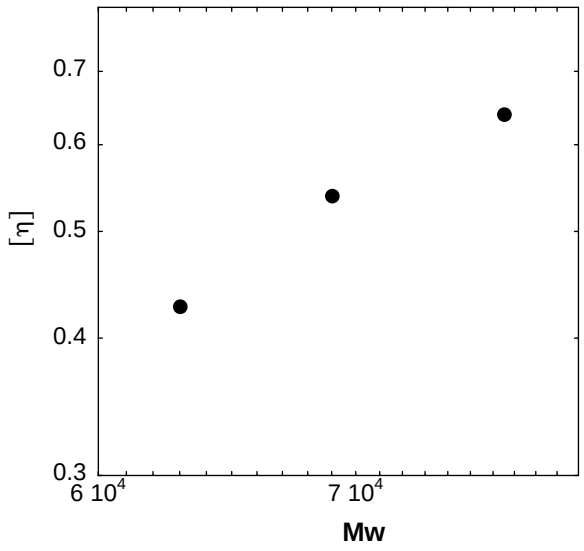

Fig. 8. Intrinsic viscosity (in dl/g) plotted against the molecular weight (in g/mol) for experimental viscometry results on a double logarithm scale.

structure because of their similar WAXD results and the fact that they are both intractable. However, because these polymers are intractable, they will not dissolve in most solvents. In order to make a qualitative comparison we carried out intrinsic viscosity measurements on the Pd catalyzed polymer. However, direct comparison is complicated by the fact that this particular polymer is not soluble in any known solvent at reasonable temperatures. Additional difficulties arise from the rapid polymerization kinetics obtained with the Pd catalyst developed by BF Goodrich. The polymerization proceeds rapidly to a relatively high molecular weight, so accurate systematic variation of the average molecular weight is somewhat difficult. To overcome the solubility issue, this Pd catalyst was used to polymerize the butyl derivative of norbornene where an *n*-butyl group was attached randomly to either carbons 5 or 6 of the norbornene monomer. Synthesis using this monomer produced a poly (norbornene) derivative soluble in 1,2,4-trichlorobenzene (TCB). To obtain a qualitative comparison for this polymer, viscometry on the alkane derivative was performed in 1,2,4 Tricholorobenzene (TCB) at the 70°C. This has been determined to be the θ condition for other polynorbornene samples using other polymerization catalysts in TCB from light scattering [18]. Its sparing solubility implies that the solvent swelling effect is small so this may be near the θ condition, however, this was not confirmed as the θ condition for this polymer made using the Pd catalyst. We shall assume that this polymer is near the θ condition because of its high barriers to backbone torsional rotation [12]. These high barriers prevent the polymer from undergoing conformational changes due to changes in solvation resulting from changes in solvent or temperature. At 70°C the polymer is locked in a particular conformation that is insensitive to the solvent and temperature (as long as the temperature is well below T_g where torsional rotation does not occurs). The fact that the chain conformation is relatively fixed implies that the polymer is always near its θ condition. This fact is consistent with the aforementioned discovery that two other isomers of poly(norbornene) with drastically different "a" exponent values both have the same θ condition (70°C in TCB) [18]. These other isomers are presumed to have different stereochemical configurations than the Pd catalyzed samples and are soluble in TCB above room temperature. TCB solutions were heated to 70°C to dissolve these polymers and light scattering coincidentally showed that the second viral coefficient was negligible indicating that this was the θ condition. The fact that this initial temperature attempted just happened to be the θ condition for two different stereoisomers implies that these polymers may be near the θ condition for a variety of temperatures.

It was also assumed that the short hydrocarbon side chains do not affect the conformation significantly because they have a minimal effect on the severe steric hindrance due to the bicycloheptane backbone. The primary effect of alkane chains appears to be to make the primary torsional minima more predominant [10]. This would suggest that the *n*-butyl derivative would have slightly higher scaling exponent of intrinsic viscosity with molecular weight than the polymer without the *n*-butyl side group. Fig. 8 illustrates that the intrinsic viscosity of *n*-butyl derivative scales with the molecular weight to approximately the power two. Using the covariance matrix from the linear regression on the plot in Fig. 8, we obtain values of 2.0 ± 0.7 and 2.0 ± 1.5 for the 80 and 90% confidence intervals on the slope, respectively. These samples were supplied by BF Goodrich, and were closely spaced due to the aforementioned difficulty in controlling the kinetics of this polymerization.

Although the comparison to experimental data is only qualitative, it suggests that the Pd catalyzed polymerization produces an erythro di-isotactic polymer because they both have an intrinsic viscosity scaling with molecular weight near the extreme value of two. Results using the MC pivot algorithm described above indicate that this scaling exponent is much lower for other stereochemical isomers of poly(norbornene) [13,14]. This discounts the possibility that all stereochemical isomers of poly(norbornene) have an "a" value near two, and qualitatively validates the hypothesis that this Pd catalyzed polymer adopts the erythro di-isotactic form.

2.4. Bulk simulations and X-ray diffraction

In molecular modeling, a polymeric glass is conceptualized as an ensemble of microscopic structures in detailed mechanical equilibrium, each microscopic structure being represented by a model cube with periodic boundaries, filled with segments from a single "parent chain" [21]. Each of the microscopic structures is in a state of mechanical equilibrium, which is a local minimum in potential energy. Molecular mechanics and molecular dynamics methods can then be used to search for these local minima. The use of local

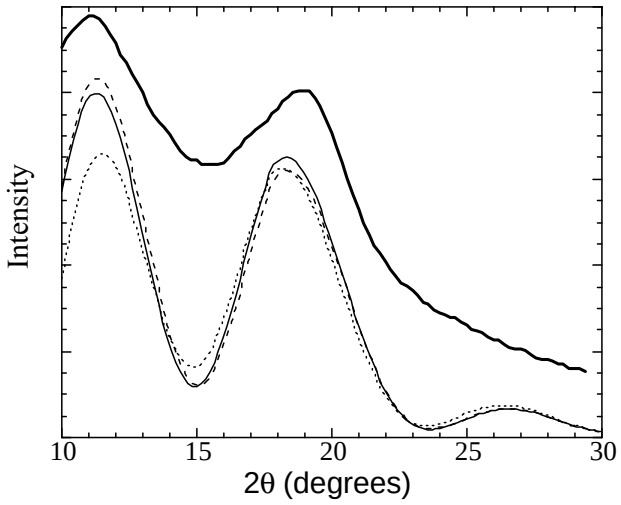

Fig. 9. Graph comparing the simulated diffraction pattern to the experimental Wide Angle X-ray Diffraction Scattering (WAXD) pattern for polynorbornene. The bold line represents experimental WAXD data [42]. The dashed line is the four chain model and the solid line is the two chain larger model. The dotted line represents simulation data for polynorbornene–polyethylene 50 : 50 random copolymer. Cu$\kappa\alpha$($\lambda = 1.54178$ Å) is used as a X-ray source for experiment and simulation.

minima assumes that glasses are not in thermodynamic equilibrium. Since local minima are sought, the minima may be expected to depend strongly on the starting conformation. Therefore, it becomes necessary to generate the starting conformation using the aforementioned RIS model. This assures that the initial conformation is consistent with the torsion angle distribution from the RIS model. This approach has been successfully used in the past to generate initial starting conformations for polymer glasses [21–23].

At present, a priori knowledge about whether the structure has been relaxed enough to be representative of the real polymer is not available, therefore, comparison with experiment is essential before the model can be used for predictive purposes. Comparing the predicted X-ray diffraction pattern to the experimental X-ray diffraction pattern allows validation of the model results. This comparison not only validates the model but also provides information about the model structure and any order or lack thereof that exists in it. Molecular mechanics methods have been successfully used to investigate the structure of a number of polymer glasses including atactic polypropylene [21], polyvinylchloride (PVC) [22] and polycarbonate (PC) [23]. On the other hand, it has been demonstrated that alternately using molecular mechanics and molecular dynamics during minimization achieves a more realistic energy minima for rigid polymers like polysulfone [39]. Therefore this is the approach used in modeling di-isotactic polynorbornene. The use of molecular dynamics only helps the minimization procedure to find a slightly improved local energy minimum, it does not accurately sample phase space in the glassy phase. It is presumed that the initial conformation is reasonable because the RIS model was used to bias the initial bulk conformation. Therefore the local energy minimum found is representative of the intermediate order in this glass.

The RIS statistical weight matrices were incorporated into the Amorphous Builder module in the Cerius$^{2®}$ software to generate isolated chains as well as chains in periodic boundary conditions. An experimentally determined density of 1.05 g/cm^3 was used for the bulk models [40]. All the results presented below represent an average taken over three different starting conformations. Four chains of 30 monomer units each constituted a single model. No statistical difference was observed within the three starting conformations at the end of the simulations. These three models were averaged to produce the dashed line in Fig. 9. Further, one model with two chains of 200 monomer units was also simulated to study the effects of model size. The isolated chains provide information about intramolecular contributions to structure, and combined with the bulk models can help isolate intermolecular contributions to the structure.

All the models were subjected to molecular mechanics minimization for 5000 steps using a conjugate gradient minimization algorithm [41], 10 ps of constant NVT dynamics at 300 K, and then subjected to minimization to a final rms force of 0.1 kcal/mol/Å. WAXD diffraction patterns simulated from the final structure, using Cerius$^{2®}$, were then compared to experimental X-ray diffraction patterns (Fig. 9). The experimental data has been taken from the work of Noll and Kaminsky using zirconocene catalyzed polymer [42]. A good comparison to experiment was observed after eliminating the small-angle component of the scattering calculated for the models using a spherical smear with a model size correction factor of 1.700 [43]. Since intensity is in arbitrary units, the experimental curve has been off-set for clarity. The important points of comparison are the relative heights of the peaks and the angle at which the peaks occur. Both sizes of poly(norbornene) models gave essentially identical results indicating that there is little sensitivity to model size.

As can be seen from the X-ray diffraction pattern for polynorbornene (Fig. 9) the first peak in the amorphous halo splits into two peaks. This corresponds to the formation of intermediate range order, which is characterized by a splitting, that occurs in the amorphous halo, typically at a wave vector magnitude of $Q = 1$ Å^{-1}. This has been previously observed in polymethacrylates [43,44] and PVC [22].In PVC the origin of intermediate range order is intermolecular, and is due to the polar interactions of the chloromethine groups [22]. Conversely, the origin of this order is more likely to be the intramolecular interactions in poly(norbornene) given the relative weakness of the intermolecular interactions.

Typically the first, or lower angle, peak in the WAXD pattern is predominantly intermolecular in nature because this corresponds to a larger interatomic distance (at $2\theta =$

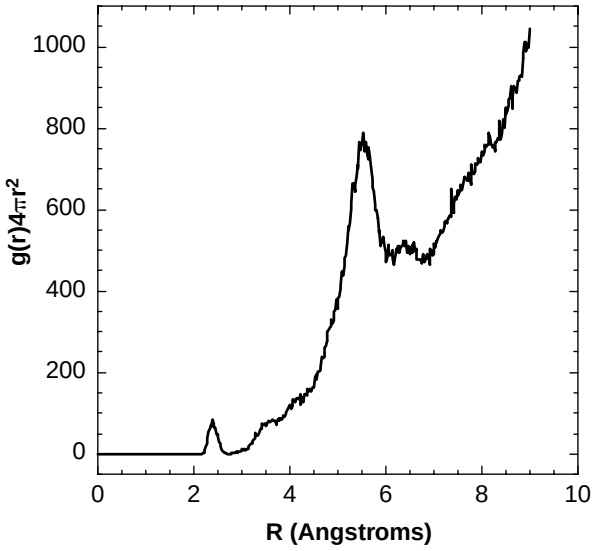

Fig. 10. Radial distribution function times the spherical volume element for bridging carbons in bulk polynorbornene models.

11, $d = 8$ Å). Likewise, the second, or higher angle peak, is predominantly intramolecular in origin and is associated with a smaller interatomic distance (at $2\Theta = 18°$, $d =$ 4.8 Å). The radial pair distribution functions $g(r)$ contain a large number of peaks and do not clearly indicate that any particular atom pair is responsible for these reflections. The radial distribution functions times their differential volume element are seen in Figs. 10 and 11 for the bridging carbon (#7) in the bulk polymer and the isolated chains, respectively. It is difficult to see any distinct pattern in these or other general radial distribution functions due to the broad distributions of atomic spacings caused by the rotation of the bicycloheptane group in the polymer. However the peak at approximately 4.8 Å in Fig. 11 indicates that at least some of the low angle peak is do to spacing

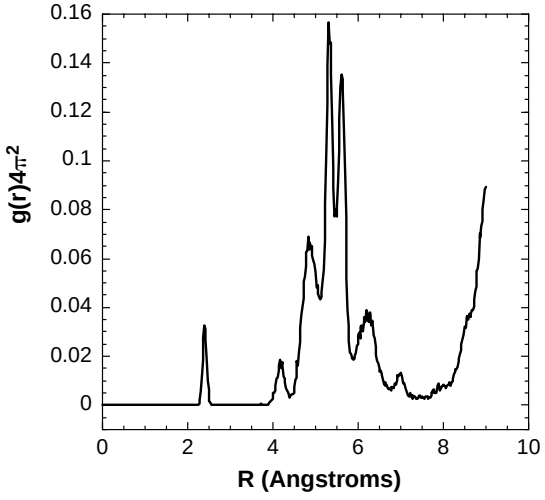

Fig. 11. Radial distribution function times the spherical volume element for bridging carbons in isolated polynorbornene chains.

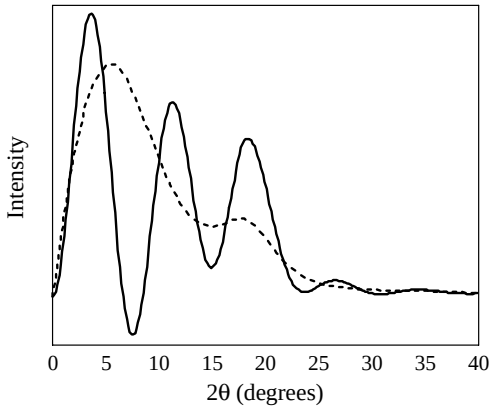

Fig. 12. WAXD pattern for isolated chains and bulk models. Solid line represents data for bulk models. Dashed line represents data for isolated chains.

within the polymer chain. Jacobson has simulated *cis* poly(*t*-butyl acetylene) in the same helical conformation predicted by our RIS model, and that produced the same two WAXD peaks seen in Fig. 9 [45]. This polymer is a useful analogue of poly(norbornene) because it has very similar conformational energetics. In its elongated form it has the identical conformation as the *cis* form of poly(norbornene) seen in Fig. 2. Also, every other backbone bond in both these polymers is non-rotatable due to the double bond in poly(acetylene) and the bicycloheptane group in poly(norbornene). The WAXD pattern for the isolated poly(norbornene) chains is contained in Fig. 12 and provides insight into what portion of the WAXD peak is intermolecular vs. intramolecular in nature. The peak at $2\theta = 18°$ in the isolated chain WAXD pattern clearly indicates that part of this high angle peak is intramolecular in nature. The lower angle peak in the bulk WAXD pattern at $2\theta = 11$ has been replaced by a broader peak at an even lower angle in the isolated chain WAXD pattern. This new lower angle peak is due to the relative increase in larger distance spacing that naturally occurs in isolated chains. In the bulk, these large distances along the polymer chains are eclipsed by the more homogeneously distributed shorter distances. The disappearance of the bulk peak at $2\theta = 11$ indicates that the lower angle peak is predominantly intermolecular in nature. This same conclusion was reached by Jacobson for his simulations of completely helical poly(*t*-butyl acetylene) by carrying out WAXD at different densities [45]. Because Jacobson's system was a symmetrically packed unit cell of aligned helices, different densities could be easily simulated without extensive regeneration of the initial chain conformation and subsequent energetic relaxation. Changes in bulk density, while preserving the helix structure resulted in significant changes to the low angle peak and negligible changes in the high angle peak. This indicated that the low angle peak is predominantly intermolecular, while the high angle peak is predominantly intramolecular. Since both Jacobson's poly(*t*-butyl acetylene) structures and our poly(norbornene) structures are dominated by the same helical conformation

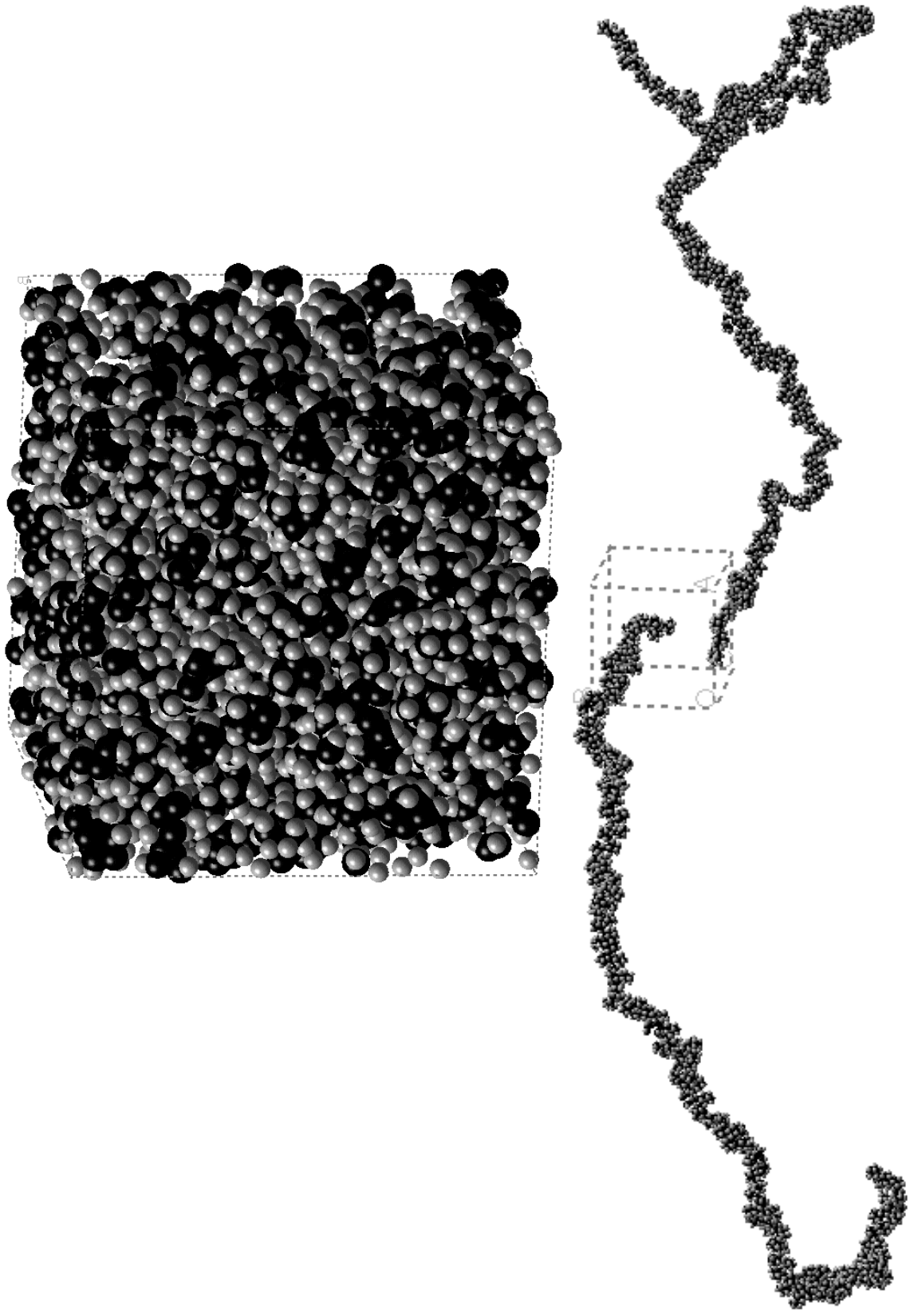

Fig. 13. Periodic and parent-chain images of the bulk simulation of poly(norbornene) with two chains of 200 repeat units. Note the helix and kink regions in the parent chain that appeared in all of the simulated chains.

this result is consistent with the above interpretation of the WAXD pattern.

In addition to the various sizes of poly(norbornene), a bulk simulation of a random copolymer of ethylene and norbornene was also simulated. The copolymer contained 50% ethylene monomers and was simulated using the same approach used for the poly(norbornene) systems. The initial guess used the aforementioned RIS model in the initial conformation generation, but the ethylene unit torsion angles were chosen randomly. The WAXD pattern resulting from an average over three simulations of four chains each with 30 monomer units for this copolymer is seen in Fig. 9. The introduction of the ethylene comonomer reduces the height of the low angle peak relative to high angle peak. The relative reduction in the low angle peak observed in Fig. 12 is approximately the same as that observed by Kaminsky in experimental WAXD patterns on such random copolymers [42].This adds additional verification that the simulated poly(norbornene) structure is reasonable.

Although many polymers form helical conformations, the helix-kink conformation proposed for erythro di-isotactic poly(norbornene) is relatively new. Some additional evidence of the accuracy of this suggested conformation is also provided by Jacobson's results on poly(*t*-butyl acetylene). While our helix-kink model accurately reproduced the experimental WAXD results, the aligned pure helical conformation suggested by Jacobson for poly(*t*-butyl acetylene) over-predicted the low angle peak [45]. The experimental WAXD pattern of poly(*t*-butyl acetylene) is almost identical to Kaminsky's measurement of the zirconocene catalyzed poly(nobornene). The ratio of the areas of the low to high angle peaks is of order 1.25 for both Kaminsky's poly(norbornene) data in Fig. 9 and for the experimental data for poly(*t*-butyl acetylene). While Jacobson's model reproduces the peak positions well, his ratio of the relative areas of the peaks is well above two. We attribute this high prediction to the fact that the pure helix model contains too much intermolecular order. The pure helix model consists of aligned helices packed closely together in a parallel fashion. Whereas the helix kink model has noticeably less intermolecular order because the kinks reduce the ability of the chain to pack in a regular fashion. Relative to the intermolecular order, the intramolecular order is not significantly reduced by the kink because most of the chain has a general helical conformation. Recall that the RIS model suggests that almost 97% of the backbone torsion angles were in the helical conformation. This helix-kink conformation can be seen in the simulated bulk poly(norbornene) systems by observing individual chains. The large, two chain, simulation is pictured in Fig. 13. The helical and kink conformations are easily seen, and the structure is qualitatively consistent with the RIS model in that much of the chain is helical in conformation. The number of kinks in all of the bulk chains occurred at a greater frequency than that suggested in the Table 1. This occurs because the effective persistence length of the polymer is much larger than the edge of the periodic cell used in the bulk simulation. Therefore, the bulk chains may be somewhat perturbed by the fact that a kink may be generated when the polymer chain runs into another periodic image of itself in this small unit cell. The persistence length cannot be quantitatively use to confirm this because of the scaling of the chain dimensions with degree of polymerization observed in this polymer causes the persistence length to diverge.

3. Conclusions

A new RIS model was developed for erythro di-isotactic polynorbornene that included long-range steric interactions that are needed to properly model its conformation. These interactions were included by extracting RIS states from an approximate energy state map for the heptamer of this polymer. The RIS model predicted a novel helix-kink conformation for this polymer in which helices were occasionally disrupted by a backbone kink. The same RIS model predicted a value of approximately 1.9 for the exponent "a" from the Mark–Houwink–Sakurada equation at the θ condition, and that $\langle r_0^2\rangle/\langle s_0^2\rangle =$ varied from 10.5 to 11.5 over a wide range of molecular weight. These RIS results were consistent with independent MC simulations. These simulations were compared with experimental results for two different poly(norbornene) polymers synthesized by Pd and zirconocene homogeneous polymerization catalysts, respectively. These two samples were presumed to have the same structure because they are both insoluble and have identical WAXD patterns. Other homogeneous catalysts produce poly(norbornenes) with very different solubilities and WAXD patterns. Viscometry experiments indicated a scaling parameter "a" very near to two for the Pd-catalyzed polymer suggesting that this polymer may be erythro di-isotactic. Although there was a fair amount of error in this value. The RIS model was utilized to create initial conformations of bulk polymers in spatially periodic cells that were energetically relaxed to produce bulk models of poly(norbornene). Accurate prediction of the WAXD pattern from these models for both poly(norbornene) and poly(ethylene-*co*-norbornene) synthesized from the zirconocene catalyst provides further evidence that these catalyst systems may produce erythro di-isotactic poly(norbornene) structures. The WAXD peak positions for these poly(norbornene) samples were very similar to those of a stereoregular poly(*t*-butyl acetylene) sample. Comparison of these simulations and poly(*t*-butyl acetylene) simulations carried out by Jacobson indicate similar conformational behavior for these two polymers. Over-prediction of the intermolecular order in poly(*t*-butyl acetylene) may occur because this polymer also has a helix-kink architecture as opposed to a perfect helix conformation used in the model. Similarities between these polymers may occur because they both have the same basic structure. Every other bond

in their backbones is essentially non-rotatable and they both contain bulky side groups.

Acknowledgements

We gratefully acknowledge the financial support of the BF Goodrich Corporation as well as the Georgia Tech Molecular Design Institute funded by the Office of Naval Research. The substantial contributions of samples and experimental analysis from Robert Schick, Brian Goodall and George Benedikt of the BF Goodrich are gratefully acknowledged. Insightful discussions with A. Abhiraman of Georgia Tech were also most valuable.

References

[1] Grove NR, Zhao Q, Kohl PA, Bidstrup-Allen SA, Shick RA, Goodall BL, McIntosh LH, Jayaraman S. Advancing Microelectronics 1996;23:16.
[2] Grove NR, Zhao Q, Kohl PA, Bidstrup-Allen SA, Shick RA, Goodall BL, McIntosh LH, Jayaraman S. IEEE Multichip Module Conference Proceedings, 1997.
[3] HOECHST Magazin Future IV. Hoechst AG, 1995;52.
[4] HOECHST Magazin Future IV. Special Science 1, Hoechst AG, 1995;32.
[5] Osan F, Hatke W, Helmer-Metzmann F, Jacobs A, Land HT, Weller T. Cycloolefinic Copolymers. In: Lecture Bayreuth Polymer Symposium, 1995.
[6] Czornyj G, Asano M, Beliveau RL, Garrou P, Hiramoto H, Ikeda A, Kreuz JA, Rohde O. In: Tummala RR, Rymaszewski EJ, Klopfenstein AG, editors. Microelectronics packaging handbook. Part II, New York: Chapman and Hall, 1997. p. 548.
[7] Kress J, Osborn JA, Ivin KJ, Rooney JJ. In: Fontanille M, Guyot A, editors. Recent advances in mechanistic and synthetic aspects of polymerization, Norwell: Kluwer Academic, 1987. p. 363.
[8] Komiya Z, Schrock RR. Macromolecules 1993;26:1387.
[9] Pierce DW, Realff MJ. Comput Chem Engng Pt B 1996;20:S1307.
[10] Haselwander TFA, Heitz W, Krugel SA, Wendorff JH. Macromolecules 1997;30:5345.
[11] Haselwander TFA, Heitz W, Krugel SA, Wendorff JH. Macromol Chem Phys 1996;197:3435.
[12] Ahmed S, Allen SA, Kohl PA, Ludovice PJ. J Phys. Chem 1998;102(49):9783–90.
[13] Ahmed S, Bidstrup SA, Kohl P, Ludovice P. Prediction of stereoregular poly(norbornene) structure using a long-range RIS model. Makromol Chem Macromol Symp 1998;133:1–10.
[14] Ahmed SA, Allen SA, Kohl P, Ludovice PJ. Computer simulation of polymers for dielectric applications. Soc Plast Engng ANTEC Meeting, May 1996;2:2179.
[15] Arndt M, Engehausen R, Kaminsky W, Zoumis K. J Mol Catal A Chemical 1995;101:171.
[16] Kaminsky W, Noll A. Polym Bull 1993;31:175.
[17] Goodall BL, Benedikt GM, McIntosh LH, Banres DA, Rhodes LF. International Patent WO95/14048,1995, (catalyst D is the palladium catalyst used).
[18] Shick R. BF Goodrich Corporation. Personal Communication, 1998.
[19] Mattice WL, Suter UW. Conformational theory of large molecules: the rotational isomeric state model in macromolecular systems, New York: Wiley, 1994.
[20] Flory PJ. Statistical mechanics of chain molecules, Oxford: Oxford University Press, 1989.
[21] Theodorou DN, Suter UW. Macromolecules 1985;18:1467.
[22] Ludovice PJ, Suter UW. In: Bicerano J, editor. Computational modeling of polymers, New York: Marcel Dekker, 1992.
[23] Hutnik M, Gentile FT, Ludovice PJ, Argon AS, Suter UW. Macromolecules 1991;24:5962.
[24] Cerius$^{2®}$. Version 2.0 published by Molecular Simulations Inc., San Diego, CA, USA, 1995.
[25] Einstein A. Ann Physik 1906;19:289.
[26] Einstein A. Ann Physik 1911;35:591.
[27] Krigbaum WR, Flory PJ. J Amer Chem Soc 1953;75:1775.
[28] Ullman RJ. J Chem Phys 1968;49(12):5486–97.
[29] Solc K, Stockmayer WH. J Chem Phys 1971;54:2756.
[30] Theodorou DN, Suter UW. Macromolecules 1980;13:506.
[31] Prager SJ. J Phys Chem 1971;75(1):72–8.
[32] Cerius$^{2®}$. Users Reference Release 2.0, BIOSYM/Molecular Simulations: San Diego, CA, USA, 1995.
[33] Metropolis N, Rosenbluth AW, Rosenbluth MN, Teller AH, Teller E. J Chem Phys 1953;21:1087.
[34] Madras N, Sokal AD. J Stat Phys 1988;50:109.
[35] Vacatello M, Yoon DY. Macromolecules 1992;25:2502.
[36] Hilstrom K. Technical Memorandum No. 297, Argonne National Laboratory Applied Mathematics Division, 1976.
[37] Baschnagel J, Qin K, Paul W, Binder K. Macromolecules 1992;25:3117.
[38] Freire JJ, Rey A, Bishop M, Clarke JHR. Macromolecules 1991;24:6494.
[39] Fan CF, Hsu SL. Macromolecules 1992;25:266.
[40] Grove N. PhD thesis, Georgia Institute of Technology, 1997.
[41] Fletcher R, Reeves CM. Comput J 1964;7:149.
[42] Kaminsky W, Noll A. Polym Bull 1993;31:175.
[43] Mitchell GR. Acta Cryst A 1981;37:488.
[44] Mitchell GR. In: Kenaith SE, editor. Order in amorphous state polymers, New York: Plenum Press, 1987.
[45] Jacobson SH. Polym Adv Tech 1993;5:724–32.